



Molecular evidence and environmental niche evolution at the origin of the disjunct distribution in three mountain endemic *Tephrosieris* (Asteraceae) of the Mediterranean basin

Martino Adamo^{1,2} · Katarina Skokanova³ · Javier Bobo-Pinilla^{4,5,6} · Elisa Giaccone¹ · Julio Peñas de Giles⁷ · Marco Mucciarelli^{1,2}

Received: 1 February 2023 / Accepted: 16 August 2023

© The Author(s) 2023

Abstract

Studies on the origin and evolutionary history of closely related plants help to understand patterns of diversity of the mountain flora in addition to providing the basis for their identification. The genus *Tephrosieris* includes three endemic taxa with small and disjoint distributions in the high mountains of the Iberian Peninsula and on the Maritime Alps. *Tephrosieris balbisiana* is native to the Southwestern Alps, *Tephrosieris elodes* to Sierra Nevada, and *Tephrosieris coincyi* to Sierra de Gredos. These taxa have been treated under different combinations of species or subspecies due to limited morphological differentiation, but comprehensive studies have not been published so far. By combining information from phylogeny, molecular dating and genome size, we demonstrated the taxonomic distinctiveness between *T. balbisiana* and the two Iberian taxa. Although the lack of variability in plastid DNA hampered the precise estimation of the diversification events, some of the recovered patterns suggested a recent divergence of *T. balbisiana*, *T. elodes* and *T. coincyi* dating back to the Pleistocene (0.5–2.8 Mya). However, niche modeling supported a geographical overlap between the three taxa during the Last Glacial Maximum (LGM). Moreover, the fragmentation of their ancient larger distribution range, particularly in the lower elevations of the Iberian Peninsula, and migration to glacial refuges in the south-western Alps, provide the most plausible explanations for the current disjoint distribution within the Mediterranean mountains. Furthermore, based on the evidence we gathered, we inferred that the alpine *T. balbisiana*, as well as the Iberian taxa, should be considered as three distinct subspecies.

Keywords *Tephrosieris balbisiana* · *Tephrosieris coincyi* · *Tephrosieris elodes* · Biogeography · Endemic flora

✉ Martino Adamo
martino.adamo@unito.it

- ¹ Department of Life Sciences and Systems Biology, University of Torino, Turin, Italy
- ² NBFC, National Biodiversity Future Center, 90133 Palermo, Italy
- ³ Institute of Botany, Plant Science and Biodiversity Centre, Slovak Academy of Sciences, Bratislava, Slovakia
- ⁴ Department of Didactics of Experimental Sciences and Mathematics, University of Salamanca, Salamanca, Spain
- ⁵ Department of Didactics of Experimental, Social, and Mathematical Sciences, University of Valladolid, Valladolid, Spain
- ⁶ Biobanco de ADN Vegetal, Edificio Multiusos I+D+I, Salamanca, Spain
- ⁷ Department of Botany, University of Granada, Granada, Spain

Introduction

The Mediterranean Basin hosts major centres of plant endemism and speciation with an exceptionally rich and diversified flora (Medail and Quézel 1999; Thompson 1999; Cañadas et al. 2014). Notably, this floristic richness thrives thanks to unique climatic and habitat conditions of this area. The unstable climate of the Pleistocene in the Cenozoic has left a fundamental imprint on the distribution and abundance of species within the Mediterranean Basin by favoring genetic differentiation, reproductive isolation and, ultimately, ecological divergence (Givnish 2010). Repeated events of speciation in allopatry followed by secondary contacts have been documented in the Iberian Peninsula (Cantabrian Range, Sistema Central, and Baetic Cordillera), the Alps (Vargas 2003; Medail and Quézel 1997; Taberlet et al. 1998; Médail and Diadema 2009; Goczał et al. 2020), and Pyrenees and

Balearic Islands (Médail and Baumel 2018; Bobo-Pinilla et al. 2022).

Genetic structure and speciation processes of the mountain flora were mainly dominated by two events (Parisod 2022). First, glacial survival during Quaternary climatic oscillations which would have prompted the in situ persistence and isolation of populations in stable climatic refugia i.e. the ice-free mountains encircled by the Mediterranean sea (Sandel et al. 2011; Christie et al. 2014; Harrison and Noss 2017; Molina-Venegas et al. 2017). Second, glacial-induced migrations to lowland or to peripheral refugia which would have allowed secondary contacts between isolated populations, followed by recolonization of alpine habitats. As a consequence of the repeated climatic oscillations, many colonization routes developed across the Southwestern Europe mountains (Vargas 2003; Dixon et al. 2009; Alárcon et al. 2012; Harrison and Noss 2017). For example, mountain ranges of the Iberian Peninsula and interjacent Pyrenees were interconnected during long glacial stages and contemporary alpine flora is the result of migration from lower altitudes after glacial retreat. However, the different cycles of range contraction and expansion experienced by mountain plants during the late Quaternary have also favored range fragmentation or the formation of temporary corridors for taxa migration (Loidi et al. 2015; Padilla-Garcia et al. 2021). Several closely related species or subspecies are now disjointly distributed across all major mountain ranges of the Mediterranean Basin (Dixon et al. 2009; Alárcon et al. 2012; Greiner et al. 2012).

The genus *Tephrosieris* (Rchb.) Rchb. comprises approximately 50 (Nordenstam 2007) perennial species with one exception—the annual *T. palustris*. Its core distribution is in the temperate and boreal zone of Europe and Asia, with a few species in the NW part of North America (Wang et al. 2009; Nordenstam and Pelser 2011). The plants of the genus are herbaceous, with erect, up to 1 m high stem not branching in the lower part; yellow to orange capitula in arranged pseudumbels or less common in panicles (Kadereit et al. 2021). The genus grows from coastal cliffs to alpine regions (up to 2500 m a.s.l.); they prefer open habitats including wet (peat bogs, the shores of lakes, ditches, or streams), mesotrophic (grasslands, tall-herb subalpine plant communities and open forests) as well as dry ones (xerophytic or rocky meadows and slopes) (Kadereit et al. 2021). Despite their close morphological resemblance, *Tephrosieris* can be easily distinguished from *Senecio* L. species without the need for microscopic examination by two easily observable characteristics: their capitula lacking outer supplementary bracts, and their styles branched with continuous stigmatic areas. Phylogenetically, the genus *Tephrosieris* is independent from *Senecio* and more closely related to *Nemosenecio* (Kitam.) B.Nord. and *Sinosenecio* as shown by previous molecular studies (Pelser et al. 2007; Wang et al. 2009).

So far, three taxa of *Tephrosieris* were identified in the Southwestern mountains of the Mediterranean Basin: *Tephrosieris balbisiana* (DC.) Holub, *Tephrosieris elodes* (DC.) Holub and *Tephrosieris coincy* (Rouy) B. Nord. The distribution of *T. balbisiana* is centred on the Mercantour-Argentera Massif, the crystalline massif located in the Maritime Alps at the border between France and Italy. Few populations can be found in northern Italy on Mount Monviso (Cottian Alps) and on the northern Apennines (Pignatti et al. 2017; Bartolucci et al. 2018). On the other hand, *T. coincy* inhabits a very small area of the western part of the Central System, Sierra of Villafranca and Sierra de Gredos (Ávila province, Central-western Spain) and a small spot in the Sanabria lake area, while *T. elodes* has only a few known localities in the south face of Sierra Nevada (southern edge of the Baetic Cordillera; southern Spain).

These short-lived perennial hemicryptophytes are typical of the high-altitude mountain flora and, all together, prefer soils with average moisture to well moistened. They belong to the vegetation of the wet grasslands and of small watercourses. *Tephrosieris balbisiana* is found mainly in subalpine tall-herb communities, also known as megaforbs, a species-rich habitat distributed along water courses at elevations as high as 2100 m a.s.l.. The community consists of a mix of tall, broad-leaved herbs thriving on soils with a relatively high nutrient status; most of these herbs are otherwise rare in open grasslands due to their sensitivity to extreme drought and grazing. However, there can be significant variations within *T. balbisiana* habitats, mainly influenced by factors such as geography, altitude, and changing soil moisture conditions throughout the vegetative season (Bono 1967; Noble and Diadema 2011). In contrast, *T. coincy* inhabits wet siliceous soils with a permanently high level of edaphic humidity throughout the year. As a result, it grows exclusively on edges of streams, mostly abandoned hay meadows, peaty meadows and small peat bogs (Martinez-Garcia 2008; Martínez-García et al. 2012). The plant can be found at altitudes ranging between 1500 and 1800 m a.s.l., although a few subpopulations are located at 1300 m and others at 1900 m a.s.l. Meanwhile, *T. elodes* belong to the oromediterranean belt and can be found only in a few watercourses within dense low-growing grasslands linked to acidic and moisture soils (hygrophilous meadow reed communities). These are communities growing on rich soils with a high-water table throughout most of the year, although not waterlogged (Molero and Marfil 2017). With only a few known localities and rapidly declining population numbers in recent decades, *T. elodes* is severely threatened (Gutiérrez et al. 2019; Peñas et al. 2019).

In a previous study, a strong genetic similarity between the three taxa was suggested (Adamo et al. 2020). This relatedness was supported by both recent (Aedo 2019) and past botanical treatments (Rouy 1890; Cufodontis 1933; Chater

and Walters 1976; Tutin et al. 1980). In 2019, Aedo treated *T. coincyi* as *T. elodes* subsp. *coincyi* (Rouy), remarking that the two can be differentiated by leaf margins which are sometimes more coarsely dentate-serrate in the former and with a broader lamina. However, Kadereit et al. (2021) proposed that morphological traits were not sufficient for the recognition of two subspecies and that both cannot be distinguished morphologically from *T. balbisiana*. Based on results of ITS and ETS sequence analysis, these authors included the two Iberian species in *T. balbisiana* (Kadereit et al. 2021), irrespective of their different distributions and habitats. More recently, Sánchez-Villegas et al. (2022) have recombined the two Iberian taxa as *T. balbisiana* (DC.) Holub subsp. *coincyi* (Rouy) P. Vargas and Luceño, and *T. balbisiana* (DC.) Holub subsp. *elodes* (Boiss. ex DC.) P. Vargas and Luceño, recognizing that both possess basal leaves attenuated and even decurrent on the petiole. In contrast, *T. balbisiana* exhibits truncated and even cordate basal leaves, with deeply toothed leaf margins. These are more often sinuate or sparsely toothed in *T. coincyi* and sometimes entire in *T. elodes* (Sánchez-Villegas et al. 2022).

Patterns of diversity of high-mountain flora are intimately linked between neighboring mountain ecosystems, such as Southwestern Alps, Pyrenees, Sierra Nevada, Apennines, Carpathians, Dinarids, and Balkans, where most of the actual alpine lineages found shelter during glaciations (Loidi et al. 2015; Kadereit 2023). It is essential for the studies to be able to predict hypothetical ancestral areas where species or their populations were in contact and how they diverged, allowing the reconstruction of possible evolutionary scenarios in order to understand patterns of diversity of the mountain flora (Parisod 2022; Nieto Feliner et al. 2023).

The main goals of this work are: (i) to better analyze the relationships within *T. balbisiana*, *T. coincyi* and *T. elodes* based on phylogeny and genome size; (ii) to reconstruct the origin of the three taxa and of their populations inhabiting mountain spots of the Mediterranean Basin using molecular dating and DIYABC analysis; (iii) to study the potential geographical contact and subsequent divergence between the three taxa using Species Distribution Modeling (SDM).

Materials and methods

Molecular analysis

Leaf material of 67 accessions of *Tephrosieris* (19 species including 6 outgroups) have been collected in nature, sampled from herbarium specimens or accessed from GenBank (www.ncbi.nlm.nih.gov/nucleotide/, last accessed 31st January 2022) (see Table 1). DNA was extracted using the NucleoSpin Plant II Kit (Macherey–Nagel, Allentown, PA, USA) following the manufacturer's protocol.

Polymerase chain reactions were carried out for two DNA regions previously identified as the most informative by Kadereit et al. (2021): for nuclear ribosomal ITS, we used the forward primer ITS7A (Jayasena et al. 2017) and the reverse primer ITS4 (White et al. 1990); for nuclear ribosomal ETS, we employed the forward primer 18S-ETS (Baldwin and Markos 1998) and the reverse primer AST1 (Markos and Baldwin 2001). PCR reactions were carried out in 25 µL volumes containing 1 µL DNA template, 5 × FIREPol[®] Master Mix (Solis BioDyne, Tartu, Estonia) 0.4 µM of each primer, and 2 µL bovine serum albumin (10 mg/mL). PCR cycles started with an initial denaturation step at 95 °C for 4 min, followed by 35 cycles of denaturation at 95 °C for 30 s, annealing at 52–58 °C for 30 s, elongation at 72 °C for 1 min, and final elongation step of 5 min. The PCR products were cleaned with NucleoSpin Gel and PCR Clean-up (Macherey–Nagel, Allentown, PA, USA) following the manufacturer's protocol and sequenced in both directions with the same primers as used for the PCRs by BioFab research s.r.l. (Rome, Italy).

Chromatograms were paired and manually checked using SeqTrace (Stucky 2012), and sequences aligned with Muscle v5 (Edgar 2004), then poorly aligned positions and divergent regions were eliminated using Gblock v0.91b (Talavera and Castresana 2007) allowing smaller final blocks and less strict flanking positions after the alignment steps ETS and ITS alignments were concatenated using SeaView v5.0.5 (Gouy et al. 2010).

Phylogenetic reconstructions were carried out with the Maximum Likelihood (ML) algorithm using RAxML v.8.2.12 (Stamatakis 2014) and with bayesian inference (BI) using MrBayes v3.2.6 (Huelsenbeck and Ronquist 2001). The concatenated alignment was found to fit the GTR + G4 substitution model using JModelTest2 (Darriba et al. 2012), ten independent RAxML bootstrapping were stopped automatically, and two independent MrBayes runs were stopped after 10,000,000 states, with a 10% burning, raising average standard deviation of split frequencies < 0.01.

The time tree was calculated using BEAST2 v2.6.6 (Bouckaert et al. 2019). Absolute age estimation analyses relied on three calibration points, strict molecular clocks, a Yule birth/death model, and a GTR + G4 substitution model. A first calibration (*Nemosenecio-Tephrosieris* MRCA) point was imposed at 3.16Mya using a log-normal distribution, the second calibration point was imposed at 8.3Mya (4.3–10.3 Mya 95% HPD [Highest Posterior Density] interval) using a log-normal distribution for the *Nemosenecio-Sinosenecio* MRCA. The third calibration point was imposed at 32.1 Mya (31.6–39.6 Mya 95% HPD interval) using a log-normal distribution for the *Doronicum-Miricaecalia* MRCA. Calibration dates were extracted from the TimeTree database (Kumar et al. 2017).

Table 1 Description of samples by accepted taxon name and collection locality of fresh material. For each sample, the NCBI accession numbers of the ITS and ETS sequences and their references are available, unless not obtained in this study. Specimen ID numbers are indicated in square brackets, when necessary

ID	Species	Locality	ITS accession	ETS accession	References
AUC2	<i>Tephrosieris papposa</i> (Rchb.) Schur	Babuna Mts, North Macedonia	MN625419	ON109687	Skokanová et al. (2019), This study
AUR2	<i>Tephrosieris integrifolia</i> subsp. <i>aurantiaca</i> (Hoppe ex Willd.) B.Nord	Veľká Fatra Mts, Slovakia	MN625399	ON109688	Skokanová et al. (2019), This study
BAL1	<i>Tephrosieris balbisiana</i> (DC.) Holub	Pian della casa, Italy	ON124720	ON109663	This study
BAL2	<i>Tephrosieris balbisiana</i> (DC.) Holub	Rio Ratisin, Italy	ON124721	ON109664	This study
BAL3	<i>Tephrosieris balbisiana</i> (DC.) Holub	Pian del Lupo, Italy	ON124722	ON109665	This study
BAL4	<i>Tephrosieris</i> sp.	San Benedetto Val Sambro, Italy	ON124723	ON109666	This study
BAL5	<i>Tephrosieris</i> sp.	Forte Geremia, Italy	ON124724	ON109667	This study
BAL6	<i>Tephrosieris balbisiana</i> (DC.) Holub	Vallone S. Bernardo, Italy	ON124725	ON109668	This study
BAL7	<i>Tephrosieris balbisiana</i> (DC.) Holub	La Lausetta, France	ON124726	ON109669	This study
COI	<i>Tephrosieris coincy</i> (Rouy) Holub	Frankfurt DNA bank [FIS-07410]	MN638859	ON109670	Skokanová et al. (2019), This study
COI1	<i>Tephrosieris coincy</i> (Rouy) Holub	Puerto de la Peña Negra, Spain [SALAF2835]	ON124728	ON109671	This study
COI2	<i>Tephrosieris coincy</i> (Rouy) Holub	Puerto de la Peña Negra, Spain [SALAF924]	ON124729	ON109672	This study
COI3	<i>Tephrosieris coincy</i> (Rouy) Holub	Arroyo del oso, Spain [SALA16302]	ON124730	ON109673	This study
COI4	<i>Tephrosieris coincy</i> (Rouy) Holub	Puerto de la Peña Negra, Spain [SALA27141]	ON124731	ON109674	This study
COI5	<i>Tephrosieris coincy</i> (Rouy) Holub	Puerto de la Peña Negra, Spain [SALA26274]	ON124732	ON109675	This study
COI7	<i>Tephrosieris coincy</i> (Rouy) Holub	Puerto de la Peña Negra, Spain [SALA25992]	ON124733	ON109676	This study
CRI3	<i>Tephrosieris crispa</i> (Jacq.) Rchb	Muránska planina Mts, Slovakia	MN625445	–	Skokanová et al. (2019), This study
DPA	<i>Doronicum pardalianches</i> L	NA	MG748399	GU818156	NA
ELO1	<i>Tephrosieris elodes</i> (DC.) Holub	Sierra Nevada, Spain	ON124734	ON109677	This study
ELO10	<i>Tephrosieris elodes</i> (DC.) Holub	Sierra Nevada, Spain	ON124739	ON109678	This study
ELO5	<i>Tephrosieris elodes</i> (DC.) Holub	Sierra Nevada, Spain	ON124735	ON109679	This study
ELO6	<i>Tephrosieris elodes</i> (DC.) Holub	Sierra Nevada, Spain	ON124736	ON109680	This study
ELO7	<i>Tephrosieris elodes</i> (DC.) Holub	Sierra Nevada, Spain	ON124737	ON109681	This study
ELO9	<i>Tephrosieris elodes</i> (DC.) Holub	Sierra Nevada, Spain	ON124738	ON109682	This study
FLA	<i>Tephrosieris flammea</i> (Turcz. ex DC.) Holub	People's Republic of China	KU696137	KU696280	Wang et al. (2009)
FOR	<i>Nemosenecio formosanus</i> (Kitam.) B.Nord	People's Republic of China	KU696044	KU696167	Wang et al. (2009)
I2	<i>Tephrosieris longifolia</i> (Jacq.) Griseb. and Schenk	Paneveggio Lake, Italy	ON124740	ON109683	This study
INA	<i>Senecio inaequidens</i> DC	San Rocco Castagnaretta, Italy	ON124742	ON109685	This study
KIR	<i>Tephrosieris kirilowii</i> (Turcz. ex DC.) Holub	People's Republic of China	AY176165	KU696281	Wang et al. (2009)
MAR	<i>Jacobaea maritima</i> (L.) Pelsler and Meijden	Turin Botanical Garden, Italy	ON124743	ON109686	This study

Table 1 (continued)

ID	Species	Locality	ITS accession	ETS accession	References
MIR	<i>Miricacalia makineana</i> (Yatabe) Kitam	Japan	GU818596	KY979011	Pelser et al. (2010), Ren et al. (2017)
PAL	<i>Tephroseris palustris</i> (L.) Rchb	People's Republic of China and Canada	MG220070	KU696283	Kadereit et al. (2021)
PAP	<i>Tephroseris papposa</i> (Rchb.) Schur	Turkey	GU818724	GU818319	Pelser et al. (2010)
PAR	<i>Parasenecio pilgerianus</i> (Diels) Y.L.Chen	Qinling Mountains, People's Republic of China	MH710824	KY978978	NA
PSO	<i>Tephroseris pseudosonchus</i> (Vaniot) C.Jeffrey and Y.L.Chen	People's Republic of China	KU696139	KU696284	Wang et al. (2009)
RUF	<i>Tephroseris rufa</i> (Hand.-Mazz.) B.Nord	People's Republic of China	AY176166	KU696285	Wang et al. (2009)
Tep10	<i>Tephroseris balbisiana</i> (DC.) Holub	Piemonte, Italy	MW779487	MW796233	Kadereit et al. (2021)
Tep11	<i>Tephroseris integrifolia</i> (L.) Holub	Bedfordshire, United Kingdom	MW779511	MW796249	Kadereit et al. (2021)
Tep12	<i>Tephroseris integrifolia</i> (L.) Holub	Wiltshire, United Kingdom	MW779512	MW796250	Kadereit et al. (2021)
Tep14	<i>Tephroseris integrifolia</i> subsp. <i>maritima</i> (Syme) B.Nord	Anglesey, United Kingdom	MW779514	MW796259	Kadereit et al. (2021)
Tep16	<i>Tephroseris integrifolia</i> subsp. <i>maritima</i> (Syme) B.Nord	Anglesey, United Kingdom	MW779515	MW796260	Kadereit et al. (2021)
Tep18	<i>Tephroseris integrifolia</i> (L.) Holub	Thüringen, Germany	MW779503	MW796251	Kadereit et al. (2021)
Tep19	<i>Tephroseris integrifolia</i> (L.) Holub	Thüringen, Germany	MW779504	MW796252	Kadereit et al. (2021)
Tep2	<i>Tephroseris coincy</i> (Rouy) Holub	Salamanca, Spain	MW779492	MW796234	Kadereit et al. (2021)
Tep21	<i>Tephroseris integrifolia</i> subsp. <i>maritima</i> (Syme) B.Nord	Anglesey, United Kingdom	MW779522	MW796261	Kadereit et al. (2021)
Tep22	<i>Tephroseris helenitis</i> (L.) B.Nord	Bayern, Germany	MW779498	MW796240	Kadereit et al. (2021)
Tep23	<i>Tephroseris helenitis</i> (L.) B.Nord	Pyrénées-Atlantiques, France	MW779499	MW796241	Kadereit et al. (2021)
Tep24	<i>Tephroseris helenitis</i> (L.) B.Nord	Languedoc-Roussillon, France	MW779500	MW796242	Kadereit et al. (2021)
Tep25	<i>Tephroseris helenitis</i> (L.) B.Nord	Navarra, Spain	MW779501	MW796243	Kadereit et al. (2021)
Tep27	<i>Tephroseris papposa</i> (Rchb.) Schur	Kosovo, Prizren	MW779521	MW796267	Kadereit et al. (2021)
Tep29	<i>Tephroseris papposa</i> (Rchb.) Schur	Greece, Ditikí Makedonía	MW779510	MW796268	Kadereit et al. (2021)
Tep3	<i>Tephroseris elodes</i> (DC.) Holub	Sierra Nevada, Spain	MW779497	MW796235	Kadereit et al. (2021)
Tep30	<i>Tephroseris papposa</i> (Rchb.) Schur	Greece, Kentrikí Makedonía	MW779520	MW796269	Kadereit et al. (2021)
Tep31	<i>Tephroseris papposa</i> (Rchb.) Schur	Greece, Ditikí Makedonía	MW779520	MW796270	Kadereit et al. (2021)
Tep32	<i>Tephroseris crispa</i> (Jacq.) Rchb	Niederösterreich, Austria	MW779493	MW796236	Kadereit et al. (2021)
Tep33	<i>Tephroseris crispa</i> (Jacq.) Rchb	Mazovia, Poland	MW779494	MW796237	Kadereit et al. (2021)
Tep34	<i>Tephroseris crispa</i> (Jacq.) Rchb	Dolny Śląsk, Poland	MW779495	MW796238	Kadereit et al. (2021)
Tep35	<i>Tephroseris crispa</i> (Jacq.) Rchb	Steiermark, Austria	MW779496	MW796239	Kadereit et al. (2021)
Tep36	<i>Tephroseris longifolia</i> (Jacq.) Griseb. and Schenk	Emilia-Romagna, Italy	MW779517	MW796264	Kadereit et al. (2021)
Tep37	<i>Tephroseris integrifolia</i> subsp. <i>serpentini</i> (Gáyer) B.Nord	Burgenland, Austria	MW779516	MW796262	Kadereit et al. (2021)
Tep38	<i>Tephroseris integrifolia</i> subsp. <i>capitata</i> (Wahlenb.) B.Nord	Alpes-Maritimes, France	MW779488	MW796245	Kadereit et al. (2021)

Table 1 (continued)

ID	Species	Locality	ITS accession	ETS accession	References
Tep39	<i>Tephrosieris integrifolia</i> subsp. <i>capitata</i> (Wahlenb.) B.Nord	Piemonte, Italy	MW779489	MW796246	Kadereit et al. (2021)
Tep41	<i>Tephrosieris longifolia</i> (Jacq.) Griseb. and Schenk	Veneto, Italy	MW779518	MW796265	Kadereit et al. (2021)
Tep42	<i>Tephrosieris integrifolia</i> subsp. <i>capitata</i> (Wahlenb.) B.Nord	Troms og Finnmark, Norway	MW779505	MW796263	Kadereit et al. (2021)
Tep43	<i>Tephrosieris integrifolia</i> subsp. <i>capitata</i> (Wahlenb.) B.Nord	Steiermark, Austria	MW779490	MW796247	Kadereit et al. (2021)
Tep44	<i>Tephrosieris integrifolia</i> subsp. <i>capitata</i> (Wahlenb.) B.Nord	Steiermark, Austria	MW779491	MW796248	Kadereit et al. (2021)
Tep45	<i>Tephrosieris integrifolia</i> (L.) Holub	Yorkshire, United Kingdom	MW779506	MW796253	Kadereit et al. (2021)
Tep46	<i>Tephrosieris integrifolia</i> (L.) Holub	Yorkshire, United Kingdom	MW779507	MW796254	Kadereit et al. (2021)
Tep6	<i>Tephrosieris integrifolia</i> (L.) Holub	Thüringen, Germany	MW779508	MW796257	Kadereit et al. (2021)
Tep7	<i>Tephrosieris palustris</i> (L.) Rchb	Alaska, USA	MW779519	MW796266	Kadereit et al. (2021)
Tep8	<i>Tephrosieris helenitis</i> (L.) B.Nord	Salzburg, Austria	MW779502	MW796244	Kadereit et al. (2021)
Tep9	<i>Tephrosieris integrifolia</i> (L.) Holub	Thüringen, Germany	MW779509	MW796258	Kadereit et al. (2021)
YUN	<i>Nemosonecio yunnanensis</i> B.Nord	People's Republic of China	KU696047	KU696170	Wang et al. (2009)

We conducted a MCMC analysis with 100 million generations with a sampling frequency of 1000 generations, the convergence of the strict molecular clock parameters was confirmed on the software TRACER v1.6 (<http://tree.bio.ed.ac.uk/software/tracer/>); all parameters had ESS > 200 (after a burn-in of 10% was removed). Maximum clade credibility trees were summarized from the MCMC trees in the program TreeAnnotator v1.8. of the software BEAST burning 100,000 initial states.

DIYABC analysis

In order to assess the evolutionary history of the three lineages, an Approximate Bayesian Computation (ABC) analysis was performed using the software DIYABC v2.1 (Cornuet et al. 2014). DIYABC calculates the posterior probabilities of alternative scenarios by simulating a large number of data sets in each case. The logistic regression procedure (Fagundes et al. 2007) estimates the occurrence of each scenario among the simulated data sets that are closest to the observed data. The aim of this approach was to compare the different phylogeographic hypotheses that could be used to explain the present distribution of the three studied lineages. Seven different sets of scenarios were designed in order to test the proposed phylogeographical hypothesis. Due to the lack of ancestral information, prior distributions of the parameters were chosen as an initial approach with a large interval. Population sizes were set equally in

all cases except for founder events. Divergence times were unrestricted to allow the program to set the most likely value. The JC69 model of nucleotide evolution (Jukes et al. 1969) was chosen, and the Uniform Mutation rate was set to $[10^{-9} - 10^{-7}]$. One million data sets were simulated for each scenario (Cornuet et al. 2008, 2010). The best scenario was chosen by calculating the posterior probabilities of each one by performing a polychotomous weighted logistic regression on the 1% of simulated data sets closest to the observed data set (Cornuet et al. 2008, 2010). Subsequent distributions of parameters were evaluated under the best scenario using a local linear regression on the 1% closest simulated data sets with a logit transformation. Confidence in the choice of scenario was tested by evaluating Type I and Type II error rates (Cornuet et al. 2010). The similarity between real data and simulated data sets was assessed for the best scenario to test the model adequacy using the posterior distribution of the parameter values.

Flow cytometric analyses

One to 15 plants per population (altogether 66 plants) of *T. balbisiana*, *T. coincy* and *T. elodes* were analyzed by flow cytometry using the fluorochrome 4', 6-diamidino-2-phenylindole (DAPI). We used fresh plant material from seedlings grown from seeds collected at the studied sites (Table S1). Each plant was analyzed separately to ensure the accuracy of relative DNA content estimations. Fresh

material of *Bellis perennis* L. ($2C = 3.38$ pg; Schönswetter et al. 2007) was added for internal standardization. The nuclei isolation and staining procedure followed the simplified two-step protocol (Doležal et al. 2007) with some modifications. First, the seedling (without the root **part**) **was chopped with intact** leaf tissue of an internal standard in 0.5 ml of ice-cold Otto I buffer (0.1 M citric acid, 0.5% Tween 20). Next, the crude nuclear suspension was filtered through 42- μm nylon mesh. For staining, 0.5 ml of a solution containing Otto II buffer (0.4 M $\text{Na}_2\text{HPO}_4 \cdot 12\text{H}_2\text{O}$), 2-mercaptoethanol (2 $\mu\text{l/ml}$) and DAPI (4 $\mu\text{g/ml}$) was added to the flow-through fraction. Samples were analyzed after 10 min incubation at room temperature. The fluorescence of 3000 particles was recorded, and only histograms with symmetrical peaks with a coefficient of variance (CV) of the standard and sample G1 peaks below 3% were considered. Flow cytometric analyses were carried out using a Cyflow ML instrument or Cyflow Space instrument (Partec, Munster, Germany) equipped with a UV-LED as an excitation source. Flow cytometric histograms were evaluated using FloMax software v2.7d (Partec, Munster, Germany). The relative DNA content was calculated as the ratio of G1 peak of standard *Bellis perennis* and G1 peak of the *Tephrosieris* sample (refer to from now on as the ratio sample/standard). The relationship between chromosome numbers and relative DNA content was verified using chromosome counts (Table S1).

A newly generated dataset of relative nuclear DNA content was compared with previously published data for hexaploid *Tephrosieris* taxa (169 individuals; Olšavská et al. 2015; Skokanová et al. 2019). Box-and-whisker plots and scatter plots were used to depict variation in the relative DNA content of the taxa studied; the Tukey–Kramer test (Tukey’s test for unequal sample size) was used to test for differences in relative DNA content between taxa. Analyses were carried out using STATISTICA 12 (StatSoft Inc. 2013).

Chromosome counting

Root tip meristems from seedlings were used for karyological analyses. The root tips were pre-treated in a 0.002 M water solution of 8-hydroxyquinoline at 4 °C for about 16 h (overnight), fixed in a 1:3 mixture of 98% acetic acid and 96% ethanol for 1–24 h, washed in distilled water, macerated in 1N HCl at 60 °C for 5 min and then washed in distilled water. Tip squashes were made using the cellophane square technique (Murin 1960). Permanent slides were stained with a 7% solution of Giemsa Stain–Modified Solution (Fluka Analytical) in Sorensen phosphate buffer, dried and observed in a drop of immersion oil using a Leica DM1000 microscope equipped with an HDCE-X5 camera and ScopeImage 9.0 software and the number of chromosomes were counted.

Species distribution models (SDMs)

We assembled a dataset of 169 occurrences of *T. balbisiana*, 33 occurrences of *T. coincyi* and 41 occurrences of *T. elodes* based on literature data, herbarium collections, personal observations, and original data from GBIF (www.gbif.org; last access December 2021) and Silene-Flore (<http://flore.silene.eu>, exported on December 2018). Occurrences for all the species were manually checked by the authors based on their own knowledge of the field, moreover, the GBIF occurrences were treated with the CoordinateCleaner R package v2.0-20 (Zizka et al. 2020) in order to remove occurrences falling into the sea, corresponding to any herbarium or research institution and other potentially problematic coordinates that might be biased by rasterized coordinates.

Due to the low number of occurrences available for the Iberian species and based on the molecular phylogeny results (see below, paragraph Phylogeny and molecular clock), we merged *T. coincyi* and *T. elodes* occurrences in a single SDM in the case of the past distributions, where models did not converge in a satisfactory way.

We calibrated species distribution models within the accessible area (Owens et al. 2013), namely the geographic extent hypothesized to fall within the long-term dispersal and colonization potential for the three modeled taxa over their evolutionary history. In the lack of precise information on the current and past dispersal ability of these species, we included all European territories between the Atlantic Ocean and the Western Alps to inspect their potential past and current interactions.

We used the 19 “standard” bioclimatic variables as predictors, all variables at a resolution of 2.5 min. Climatic variables were downloaded from WorldClim2 (Fick and Hijmans 2017) for the “current” period (1970–2000), the Last Interglacial (LIG; ~120,000–140,000 years ago) (Otto-Bliesner et al. 2009) and the Last Glacial Maximum (LGM, ~22,000 years ago). In the LGM case, we used the three models CCSM4 (Gent and Danabasoglu 2011), MPI-ESM-P (Xu et al. 2018) and MIROC-ESM (Watanabe et al. 2011). We decided to focus on climatic predictors, excluding soil features. This choice was guided by the high collinearity level observed between climate and pedology in mountain ranges (Adamo et al. 2020), moreover, it has been observed that when assessing climate change impact, the number of predictor variables in SDMs should be kept reasonably small in order to obtain models of higher quality (Brun et al. 2020). Hydrological systems topography or habitats were not used as predictors or to calibrate the SDMs. Habitats occupied by our species are sized at a local scale, while the calibration of the model is at regional scale.

The current climate is important for species conservation, but also to visually check the goodness of fit of our models, since the great majority of the species stations, are actually

included in the analysis. Niche distributions in past cold and warm periods were modeled in order to ascertain potential contacts between the three taxa.

We explored predictors' importance on both presence and pseudo-absence points using a Principal Component Analysis (PCA); we tested collinearity between predictors (Braunisch et al. 2013) using Pearson correlation, setting the threshold for collinearity at $|r| > 0.7$ (Zuur and Ieno 2016). We excluded collinear variables based on our expert opinion, moreover, we used PC1 and PC2 as proxies for predictors prioritization (Guisan et al. 2017).

To model species distribution, we used four different probabilistic models found in the 'biomod2' package in R (Thuiller et al. 2021): Generalized Additive Model (GAM), Generalized Boosting Model (GBM), RandomForest (RF) and Classification Tree Analysis (CTA). We ran the models with two different sets of pseudo-absence points ten times more abundant than presence points. Each model was then calibrated using 70% of each presence/pseudo-absence dataset and evaluated with the 30% remaining. We evaluated the model's predictive accuracy using two different indices: the True Skill Statistics (TSS, Allouche et al. 2006) and the area under the receiver operating characteristic curve (ROC, Hanley and McNeil 1982).

We projected the model into the accessible area to obtain a graphical representation of the current potential bioclimatic niche suitability of *T. balbisiana*, *T. elodes*, and *T. coinnyi*, and the past bioclimatic potential niche of *T. balbisiana* and of *T. elodes* together with *T. coinnyi*. In the case of the LGM prediction, we settled at zero suitability for the areas covered by glaciers (and nunataks) using the ice distribution by Ehlers et al. (2011).

Results

Phylogeny and molecular clock

RAxML, MrBayes, and BEAST topologies were almost identical, but with different branch supports, thus we reported the single consensus tree obtained with MrBayes. In the BI analysis of combined ITS and ETS sequences (Fig. 1), three major clades were resolved. The "integrifolia clade" (node support 87/1.0 for Maximum Likelihood and Bayesian analysis, respectively) which contains *T. integrifolia* and *T. palustris* sequences as sisters to the former. All the subspecies of *T. integrifolia* were included in this single clade. The "longifolia clade" with *T. longifolia*, *T. helenitis*, *T. papposa*, and *T. crispa* which are not monophyletic. The clade support was high only in the case of the Bayesian analysis (52/1.0, respectively). The "longifolia clade" included two sequences from samples collected on the northern Apennines by Adamo

et al. (2020) that are regarded as belonging to *T. balbisiana*; here named *Tephroseris* sp. BAL4 and BAL5. The "T. balbisiana clade" (node support 85/1.0) contains the sequences of *T. balbisiana*, *T. coinnyi* and *T. elodes*. Inside it, we retrieved a well-supported separation between *T. balbisiana* (node support 87/1.0) and the two Iberian taxa (node support 91/1.0). According to this finding, here we propose to recognize them as separate subspecies of *T. balbisiana* (see Discussion for more details). Iberian taxa, however, formed a polytomy including among the others, sequences of *T. elodes* samples collected in the field for this study and the sequence (Tep3) of the specimen at the Berlin Herbarium (Kadereit et al. 2021). Our phylogeny strongly supported four clades: longifolia, integrifolia, *T. balbisiana*, and Asian (all nodes supports were 1.00 in the bayesian analysis). We found a good support for the relationship between the longifolia and integrifolia clades (0.95), while the node for the *T. balbisiana* and Asian clades was weakly supported (31/0.59).

Time tree analysis reports ranges of time in million of years only for the nodes showing supports higher than 70/0.75 (Fig. S1). *Tephroseris* genus separated from the sister genus *Nemosenecio* at about 6.73 [8.29–5.33] Mya. Divergence of the integrifolia and longifolia clades from the Asian and *T. balbisiana* clades dated at 4.61 [5.88–3.55] Mya. The node at the separation between the Asian and *T. balbisiana* clades was unsupported according to ML and Bayesian analysis. However, we were able to date the separation between *T. balbisiana* subsp. *balbisiana* and the clade with *T. balbisiana* subsp. *coinnyi* and *T. balbisiana* subsp. *elodes* at 2.56 Mya [3.7–1.6] (Fig. S1).

Results of the DIYABC analysis

Of all the scenarios tested, the three with the highest statistical support were Scenario 4 which received the highest posterior probability [$P_4 = 0.28$ (95% CI 0.23–0.31)], followed by Scenario 3 and Scenario 1 [$P_3 = 0.18$ (CI 0.14–0.20) and $P_1 = 0.17$ (CI 0.14–0.19)] (Fig. 2). Scenario 4 supported the derivation of *T. balbisiana* and *T. elodes* from a common ancestral population. This event would have been followed by the more recent divergence of *T. coinnyi*. Scenarios 3 showed *T. elodes* as diverged from an ancestral population of *T. balbisiana* (Scenario 3), while *T. balbisiana* as diverged from an ancestral population of *T. elodes* (Scenario 1).

For Scenario 4, Type II error rate (the probability that a Scenario was selected when it was not the true Scenario for the simulated data) and Type I error rate (the probability that it was not selected when it was the actual Scenario) were 26% and 41%, respectively, owing to the high similarity among scenarios.

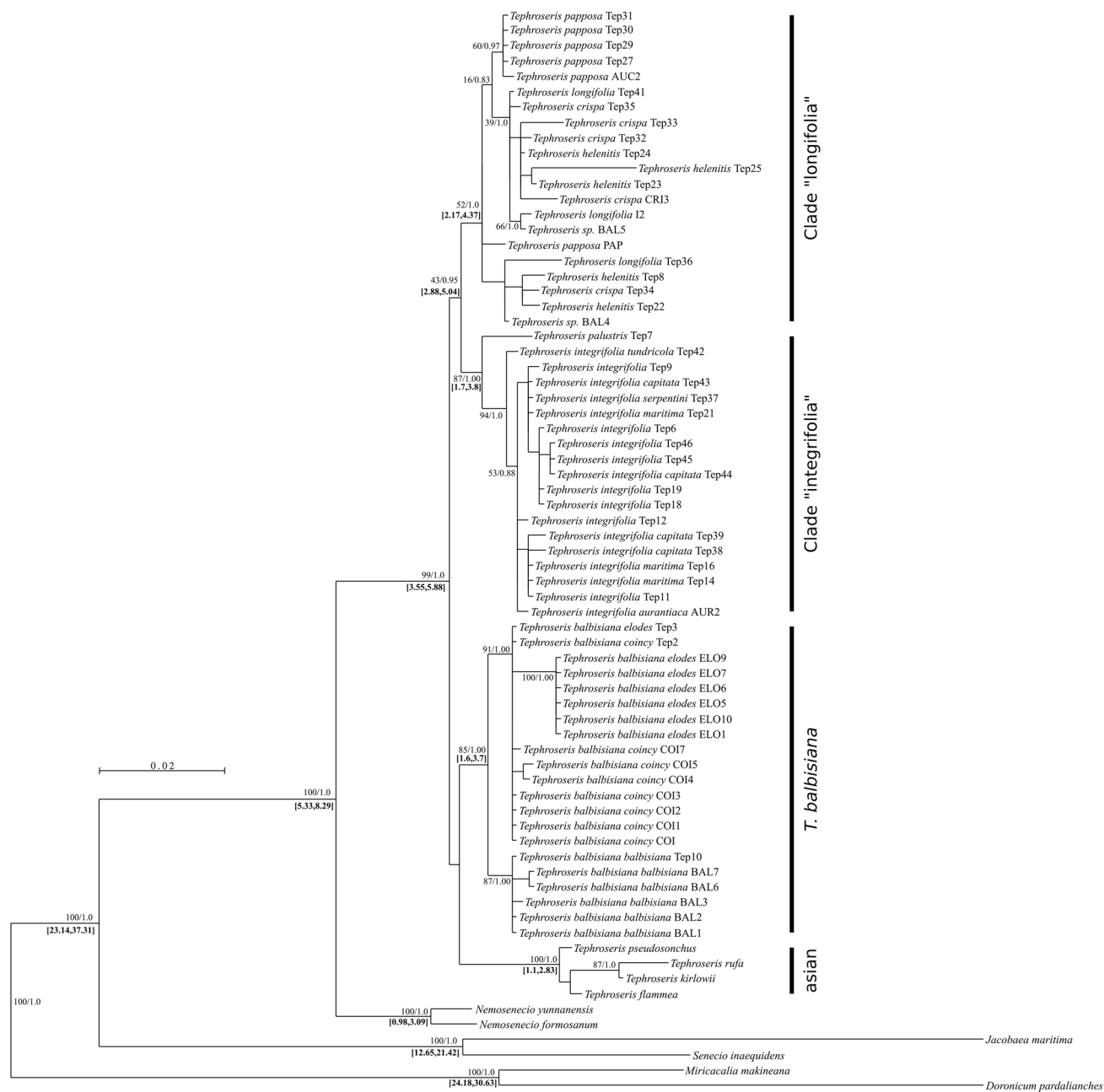


Fig. 1 *Tephroseris* genus phylogeny based on ITS and ETS regions. The tree topology corresponds to results of the Bayesian inference. Numbers at nodes over the branches report maximum likelihood bootstrap values and posterior probabilities, respectively. Node supports are reported when bootstrap was higher than 70 or posterior probability higher than 0.85. Square bracketed bold values below nodes correspond to the 95% HPD intervals, namely, the most probable split time between taxa. 95% HPD intervals are reported only

Karyological analyses and relative DNA content

The chromosome number $2n = 48$ was newly reported for *T. elodes* and *T. balbisiana*, and $2n = 48 + 1B$ for *T. coincy* (Fig. S2, Table S1). Relative DNA content estimates of

for supported nodes. Labels correspond to accepted name of taxa, followed by an ID corresponding to those in Table 1. We identified “integrifolia clade” and “longifolia clade” as highly supported clades (continuous line), while “Asian clade” and “*T. balbisiana* clade” were not appropriately separated, thus, since the inner nodes were well supported, we choose to keep the separation as a partially supported clade (dashed line)

T. balbisiana, *T. coincy* and *T. elodes* corresponded to a hexaploid level $2n \sim 6x \sim 48$ (Table S1). Relative DNA contents significantly differed between the two Iberian populations (P.to Peña Negra and Sierra Nevada) and were significantly higher than those measured in populations sampled

for *T. balbisiiana* (Tukey–Kramer, $P < 0.001$) which, conversely, did not significantly differ (Fig. S3) pointing to a single species. Interestingly, the Iberian species, *T. coincyi* and *T. elodes*, showed relative DNA contents significantly higher also with respect to all the remaining European hexaploid *Tephrosieris* (data obtained from Olšovská et al. 2015 and Skokanová et al. 2019) as represented by box-and-whisker plots (Tukey–Kramer test, $P < 0.05$) (Fig. 3). Notably, according to this last comparison, *T. balbisiiana* and *T. longifolia* subsp. *gaudini* did not differ for their DNA contents (Fig. 3).

Climatic features of the three mountain *Tephrosieris*

We built models based on five non-collinear variables, namely Isothermality (bio3), Temperature Seasonality (bio4), Mean Temperature of Wettest Quarter (bio8), Annual Precipitation (bio12), and Precipitation of Warmest Quarter (bio18). PCA highlighted the overlap between bioclimatic hypervolumes of *T. coincyi* and *T. elodes*, while *T. balbisiiana* belongs to a clearly independent bioclimatic hypervolume (Fig. S4). All models converged pointing to bio8, the mean temperature for the 3 months with the highest cumulative precipitation, as the most important predictor of the distribution of the two Iberian species. Conversely, the most important predictor of *T. balbisiiana* distribution was isothermality (bio3) in GAM, GBM, and RF, while in CTA the most important variable was the mean temperature of the wettest quarter (bio8), followed by bio3 (Table S2).

Coherently with PCA observations, predicted models showed that the three taxa have similar but not identical climatic features. As expected in consideration of their mountain ranges, habitats of the three taxa are characterized by marked temperature changes over the course of the year (bio4) (Fig. S5), and this was true especially in the case of *T. elodes* habitat which would show major climatic

extremes. This finding is supported also by the observation that *T. coincyi* and *T. balbisiiana* habitats would be characterized by narrower diurnal temperature oscillations (bio3) than in the habitat of *T. elodes*. Mean temperatures in the wettest quarter (bio8) are around zero or lower for all the three taxa. Total annual precipitation (bio12) resulted particularly important for *T. balbisiiana*, in fact, this species shows a peak of suitability for sites characterized by ~ 1000 mm of rain per year, a value which can be significantly lower in the case of the Iberian taxa. Consequently, precipitations in the warmest quarter of the year (bio18; the less rainy quarter in all three cases) range between 150 and 180 mm in *T. balbisiiana* habitats, while the two Iberian species would prefer drier summers (Fig. S5).

Current and past bioclimatic potential niches

Model's predictive accuracy estimated with ROC and TSS were interpreted using the classification of Araújo et al. (2005), and indicated excellent model performances (Fig. S6), resulting in scores higher than 0.8 for all the estimations associated to restrained standard deviations. Projections of the potential distribution of the three taxa into the current climate conditions over-impress the known distribution of the three taxa, highlighting a core area extending over the Ligurian and the Maritime Alps as well as over Sierra Nevada and Sierra de Gredos, where *T. balbisiiana*, *T. elodes*, and *T. coincyi*, respectively, grow. In the Lago de Sanabria area, where *T. coincyi* can also be found, we predicted lower niche suitability, if compared to the above-described core ranges (Fig. S7).

The model predicted a few areas with high niche suitability, where the species are not currently present or documented, namely: Baza-Los Filabres range mountain for *T. elodes* and a series of elevated regions in the North direction for *T. coincyi*.

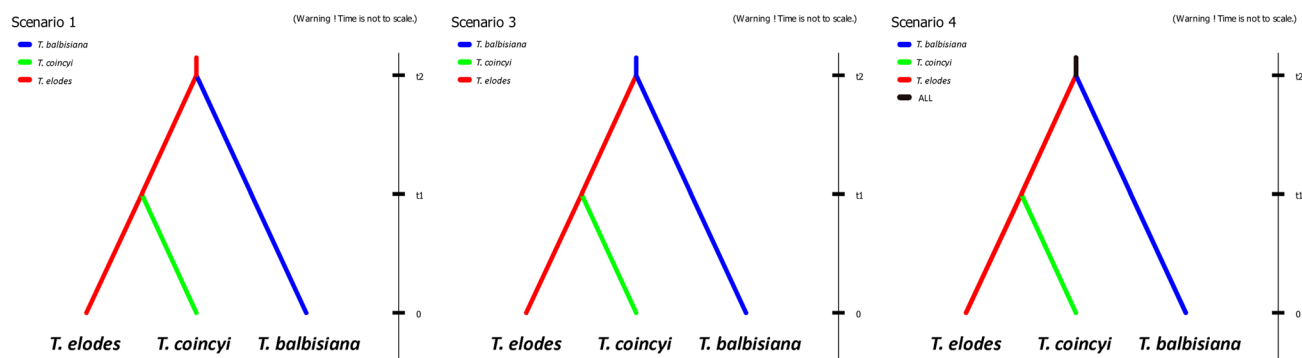


Fig. 2 Hypothetical coalescent scenarios tested in DIYABC for the evolution of the three endemic *Tephrosieris*. Statistically, Scenario 4 was the most probable, assuming the presence of a common ancestor for the Alpine and the Iberian branches. Scenario 1 and Scenario 3

had lower, but similar probabilities. Scenario 4 assumes that *T. balbisiiana* and *T. elodes* diverged at the same time from an ancestral population and that the Iberian *T. coincyi* had diverged only later. All the remaining Scenarios had a low probability to be actual ($P < 0.15$)

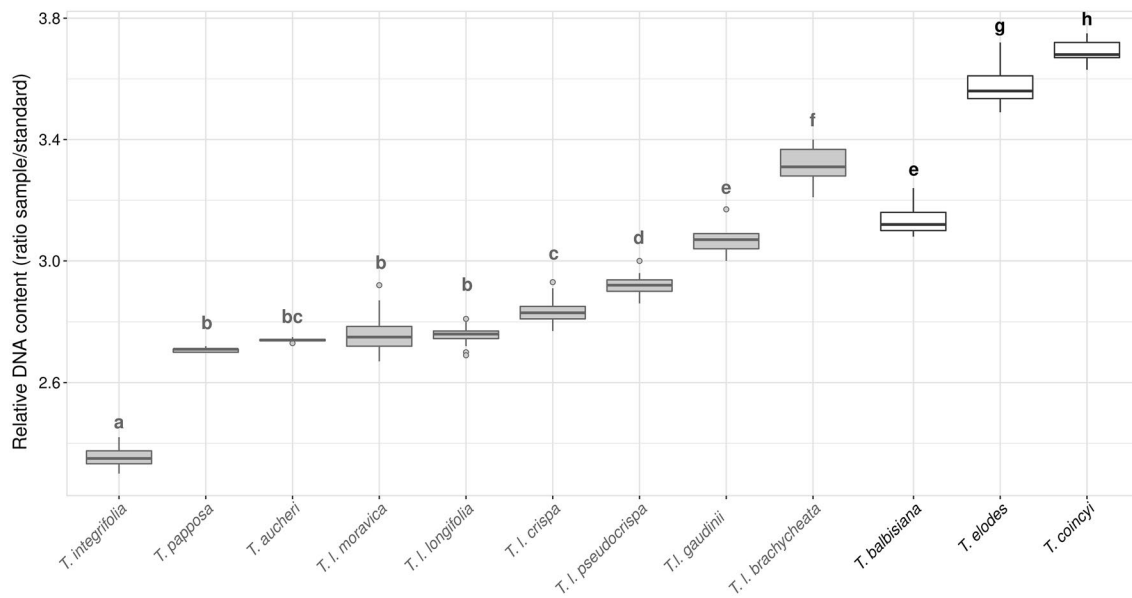


Fig. 3 Relative DNA contents of the hexaploid *Tephroseris* taxa (see Table S1 for details). Statistically significant differences (Tukey–Kramer, $P < 0.05$) were reported by different small letters. Grey box-

plots correspond to bibliographic data (Olšovská et al. 2015; Skokanová et al. 2019), while black boxplots are from this study

To project the potential distribution in the past of the three *Tephroseris* taxa, we merged *T. elodes* and *T. coincyi* occurrences. At LIG conditions, the Iberian taxa showed scattered occurrences across the Iberian Peninsula and very similar to their actual distribution. *T. balbisiana* optimal distributions corresponded to the French northwestern Alps, with the addition of a restricted area of niche suitability located on the Pyrenees (Fig. 4).

Tephroseris distributions during LGM differed from those projected for LIG and current climate conditions. According to the models, niche suitability would have generally expanded and moved toward areas at lower altitudes in the French Central Massif and in the Iberian Peninsula, probably dominated by warm temperatures and lower precipitations. *T. balbisiana* optimum of distribution shifted in a southeastern direction and it was mainly centered on the Northern Apennines (Fig. 4). Expansion of distributions at lower elevations in the Iberian Peninsula would have allowed for the establishment of interconnections between populations at all major sites presently occupied by *T. elodes* (Sierra Nevada) and by *T. coincyi* in the Central System (Sierra of Villafraña and Sierra de Gredos) (Fig. 4). Moreover, *Tephroseris* distribution would have shown also a shift toward the lower elevations bordering the Pyrenees and to the Massif Central of France. Following the linear arrangement of the main mountains of Southwestern Europe, *Tephroseris* distribution would have further extended to the Southern Alps and the Northern Apennines (Fig. 4). This finding is likely to enforce the preference for climatic patterns of Southern Europe and particularly for the climate of coastal

(sea-mitigated) mountain ranges which could have behaved as peripheral refugia during the LGM (Fig. 4). During the last 20,000 years, a substantial reduction of *T. balbisiana*, *T. elodes* and *T. coincyi* ranges occurred (~92%, ~97% and ~97%, respectively). *T. balbisiana* distribution shifted from the Northern Apennines to the current distribution on the Southwestern Alps by the end of the LGM. In addition, the habitat of the Iberian species would have contracted into the current disjointed ranges (pale blue area; Fig. 5).

Discussion

By combining molecular and genome size data with information on ecological niche evolution, we assessed the taxonomic distinctiveness and the diversification history of three *Tephroseris* endemic to the Mediterranean mountains. Overall, we find that results of phylogeny and molecular dating may be congruent with a recent divergence of *T. balbisiana*, *T. elodes* and *T. coincyi*, as already reported for the other European taxa (Kadereit et al. 2021). Climatic preferences and patterns of niche evolution supported a geographical overlap of the three taxa in LGM. Limits of the nuclear DNA sequences and the lack of variability in plastid DNA weaken our ability to date precise sequences of events in their diversification. However, some of the recovered patterns were congruent between analyses, allowing us to draw some general conclusions on the evolutionary patterns and taxonomic asset of *Tephroseris* within the Mediterranean mountains.

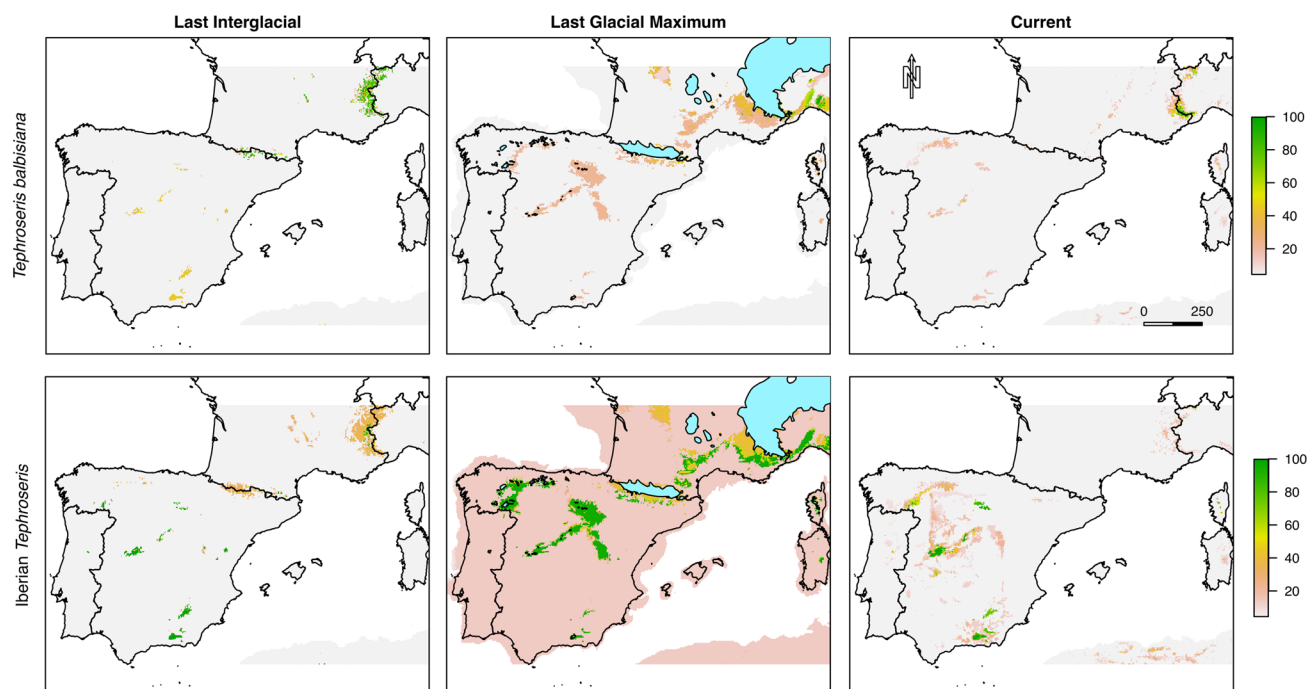


Fig. 4 Distribution prediction of *Tephroseris balbisiana* (the three upper maps) and the Iberian *Tephroseris* (all together in the three lower maps) for the Last Interglacial period (LIG; first column), the Last Glacial Maximum (LGM; second column), and current time (third column). Color gradient axis on the left of figures goes from

gray to green and represents growing level of habitat suitability for *Tephroseris*. Pale blue areas in the LGM models represent maximum ice shield expansion during LGM. North arrow indicates the orientation in the maps, while the scale bar refers to km; for simplicity, these frames are reported only once in the *T. balbisiana* current SDM

Phylogenetic relationships

Based on rDNA spacers (ITS and ETS), European species of *Tephroseris* grouped into two supported clades separated by the Asian clade, largely confirming previous studies (Skokanová et al. 2019). The novelty of our analysis was the clade with *T. balbisiana*, *T. coyinci* and *T. elodes* and their separate placement from all the other European taxa (Fig. 1). *Tephroseris balbisiana* genetic asset had never been deeply inspected so far. Using sequences from different populations living in Mercantour-Argentera Massif at the core of the Maritime Alps and on the main mountains of Iberia, we were able to show a very well-supported separation between the sequences of *T. balbisiana* and the two Iberian taxa and to propose the recognition of the three taxa as separated subspecies. Only three individuals were used before to analyze the entire “balbisiana” clade (Kadereit et al. 2021), and this approach might have led the authors to conclude that these sequences corresponded to a single species with a largely fragmented range. In our study, the exclusion from the “balbisiana” clade of two sequences (BAL5 and BAL4; Fig. 1) originating from the Northern Apennines (almost probably erroneously ascribed in previous studies to *T. balbisiana*; Bonafede et al. 2013) would stress the distinctiveness of the

populations of the Maritime Alps and enforce the role of this geographic area as a center of endemism for the genus.

Relative genome size and chromosome numbers

Results of this study showed important differences between the Iberian and the Alpine *Tephroseris*, pointing to the existence of at least two distinct genome size lineages (Fig. 3 and Fig. S3). No other *Tephroseris* species, in fact, has a genome size as high as *T. coyinci* and *T. elodes*, a finding that might imply the evolutionary isolation of the Iberian populations. However, the significant differences in genome size found between the two Iberian taxa would argue for their recognition as two subspecies. Overlapping genome sizes found between populations of the Maritime Alps supported, on the other side, the existence of a single genetic pool on this mountain range. Moreover, the fact that *T. balbisiana* genome size lies between those of *T. l.* subsp. *brachychaeta* and *T. l.* subsp. *gaudinii* would imply a relatedness of the alpine species to the *T. longifolia* aggregate of species (Adamo et al. 2020). If this finding was proven, an older dating of *T. balbisiana* with respect to *T. coyinci* and *T. elodes* will find support.

The chromosome count of $2n=48$ was newly reported for *T. balbisiana*. Similarly, the re-examination of *T.*

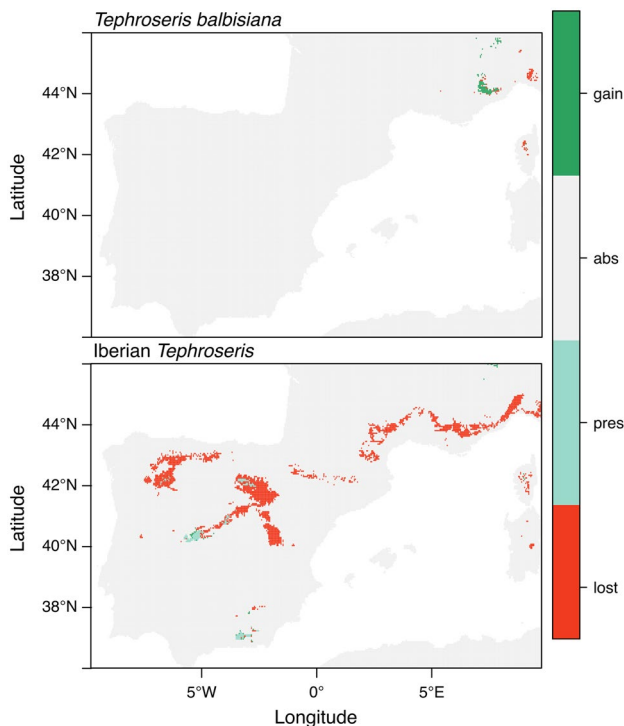


Fig. 5 Loss (red) and gain (green) of habitat suitability predicted for *T. balbisiana* and the two Iberian taxa, comparing the habitat predicted for the LGM with current suitability. A shift can be observed in the *T. balbisiana* distribution from the Northern Apennines to the current distribution on the Southwestern Alps (green dots). According to the model, Iberian species would have lost a very large portion of their species range because of ice retreat and have contracted into current disjointed ranges (pale blue area)

elodes from Sierra Nevada revealed chromosome number of $2n = 48$, which contradicts the previous record $2n = 40$ (Blanca and Cueto 1992) from the same site/mountain range. When Kadereit et al. (2021) revised the voucher specimen of the record by Blanca and Cueto (1992), they ruled out its incorrect identification. However, the possibility of miscalculation or aneuploidy should be considered. Previously, the chromosome counts of $2n = 40$ for any *Tephroseris* taxa have been considered unusual because the lowest chromosome number reported for many species of the genus was $2n = 48$ (Kochjarová 2005; Altınordu et al. 2014; Kadereit et al. 2021). Nevertheless, aneuploidy has been known in the genus such as the chromosome number of $2n = 46$ has been reported for *T. integrifolia* subsp. *aurantiaca* (Liu and Yang 2011).

Climate preferences and climatic niche evolution

Our results showed that niche suitability in *Tephroseris* retreated to high altitudes during the interglacial period (LIG was characterized by a climate warmer than present day) and, converse, niche expanded toward lower altitudes

during the Last Glacial Maximum (LGM; cold climate, approximately 22,000 years ago). Similar altitudinal variations of species niche have been documented for the flora of the Maritime Alps, of the mountain massifs of the Iberian Peninsula and in Pyrenees (Martín-Bravo et al. 2010; Peredo et al. 2009; Guerrina et al. 2022). In the Iberian Peninsula, high temperatures during LIG, impaired the survival of cold-adapted species at low altitudes. For example, temperature increase during LIG has forced Iberian populations of *Erodium* to migrate northward or to remain isolated on high mountains (Alárcon et al. 2012). On the contrary, given the limited ice extent in Central Iberia, some cold-adapted endemics as *Androsace vitaliana* (L.) Lapeyr. underwent a massive range expansion during the LGM and migrated to lowlands (Boucher et al. 2012). Diversification in this taxon would have involved long-distance dispersal during the Pleistocene trough connections existing between the Alps and the mountain systems of the Iberian Peninsula bypassing the Pyrenees (Dixon et al. 2009). Our projections of SDMs at the LGM, however, tell a slightly different story when comparing *T. balbisiana* and the two Iberian taxa. In response to LGM, the niche suitability of the cold-adapted Iberian taxa significantly increased due to improved temperature trends at lower altitudes. Additionally, the minimal extent of ice during this period preserved the original distribution of *Tephroseris* populations in the higher mountains of Central Iberia. Furthermore, the extension of the ice shield forced the populations of *T. balbisiana* to shift from the western Alps toward southern ranges such as glacial refuges of the Maritime Alps and, possibly, the Northern Apennines. Conversely, the populations of *Tephroseris* of the Iberian Peninsula experienced a more extensive range expansion. Therefore, it seemed that their habitat suitability extended toward Pyrenees, the Central Massif, possibly even the Southwestern Alps (Fig. 4).

Our results showed that the three taxa have similar climatic niches, specifically preferring habitats with high levels of soil humidity during the vegetative stage. *Tephroseris balbisiana* has a higher requirement for total annual rainfall compared to the Iberian *Tephroseris*, which, in contrast, thrives in soils with consistently high levels of edaphic humidity. These features could have evolved after the establishment of *Tephroseris* populations on their current habitats at the end of the LGM. Consistent with the findings of Pellisier et al. (2013) and of Wasof et al. (2015), geographically isolated populations tend to conserve their ecological niche over time spans of millennia. This tendency is particularly pronounced in species that prefer cold temperatures and moist soils, which could also apply to *Tephroseris* after fragmentation of its range across the Mediterranean mountains.

Post-glacial contraction has been mainly explained by intolerance of cold-adapted species to warmer temperatures and the increase in competition by larger plants (Birks 2008;

Martín-Bravo et al. 2010). According to our model, a considerable reduction of the niche suitability was predicted for the Iberian species which, after ice retreat, would have lost a very large portion of their range and contracted into current disjointed ranges (Fig. 5).

Population divergence history and molecular dating

It is likely that LGM saw the spread of *Tephroservis* within a large geographic area, potentially corresponding to the mountains within current Mediterranean bioclimatic region. This interpretation seems to find support by results of the DIYABC analysis which showed derivation of both Iberian and Alpine *Tephroservis* from a common ancestor no longer extant (Scenario 4, Fig. 2). From the end of the LGM to the early Holocene (11,000 years before present), because of the warming of the Mediterranean climate, *Tephroservis* range would have ultimately undergone a strong contraction and a multiple fragmentation during the retreat of the ice (Figs. 4 and 5). This occurrence would have led to the current distribution of three schizo-endemic taxa: *T. balbisaniana*, *T. coincyi* and *T. elodes*, isolated into their relict mountain ranges (Diadema et al. 2005; Schmitt et al. 2010). The geographical divergence within Mediterranean *Tephroservis* in relatively recent times as a result of fragmentation processes separating populations from Iberia and the Alps is seemingly in contrast with the results of our molecular clock which pointed to the split from the ancestor of the “*T. balbisaniana*” clade dating well before the Quaternary glacial series (1.6–3.7 Mya; Fig. S1). However, results of our molecular dating are congruent with previous literature. (Skokanová et al. 2019). As hypothesized by Skokanová et al. (2019) and by Kadereit et al. (2021), in fact, main diversification events within the European taxa of *Tephroservis* likely took place in the Pleistocene (0.5–2.8 Mya) under the action of glacial cycles which led to migration and subsequent isolation into southern refugia of central and subalpine European populations. According to our phylogenetic data and Skokanová et al. (2019) and Kadereit et al. (2021), *T. balbisaniana* group diversification would have happened in (Pliocene-) early Pleistocene. After that, Pleistocene glacial circles forced the populations to “get closer” geographically (and ecologically) as in our LGM projections, and had compatible contacts (once or more times). Geographical separations in interglacial altering periods (as in our LIG projection, and others before), probably also happened even if with low genetic divergences because of conservative ecological niches. This interpretation supports main diversification events within “*integrifolia*” and within “*balbisaniana*” at about 1.6–3.8 Mya and those within “*longifolia*” clade, slightly earlier (about 2.17–4.27 Mya). We are aware, however, that the complete lack of variability found in plastid DNA for the three taxa could have limited a precise dating of diversification events

(Pelser et al. 2010), forcing our analysis to be circumscribed to the ETS and ITS spacers.

Alternatively, the Iberian *Tephroservis* would not have expanded to reach the south-western Alps during the LGM. Indeed, Pyrenees together with Sierra Nevada and the Alps are regarded as the sole three main areas covered by ice in Southern Europe during the LGM (Ehlers et al. 2011). As addressed by the result of DIYABC, Iberian and Alpine populations extending their range during the LGM (Fig. 4 LGM), would have come in contact and genetically admixed on the Pyrenees (likely, all three Scenarios of Fig. 2 are compatible with this view). Pyrenees have been regarded as a geological barrier to postglacial colonization from southern Iberian refugial areas as well as a migratory northward route (Taberlet et al. 1998). Yet, according to the projection model performed by Garcia-Ruiz et al. (2003), ice covering is estimated to have descended as down as 900 m a.s.l. in the Pyrenees and 1200 m a.s.l. in the Pre-Pyrenees. Thus, “bridging” populations of *Tephroservis* would have occurred in the low-altitude western and eastern edges of the Pyrenean range (Padilla-Garcia et al. 2021) (Fig. 5). The persistence of mountain populations in the Central Pyrenees is likely to have been hampered by the harsh conditions at the higher elevations, possibly explaining also the current absence of *Tephroservis* from these mountains.

According to this scenarios, evolutionary processes at the base of *Tephroservis* diversification would infer the importance of the biogeographical relationships between different areas of the Mediterranean Basin (Western Alps, Pyrenees, and Iberian Massifs) hosting different processes of migration and isolation. These last evolutionary events, yet to be demonstrated, would find support in the results of genome sizing conducted on the three taxa.

Proposed taxonomic treatment and conservation consequences

Phylogenetic studies have shown that the European species of *Tephroservis* are characterized by low evolutionary rate, particularly in relation to plastidial DNA (Adamo et al. 2020; Kadereit et al. 2021). Despite sequencing the plastome of *T. balbisaniana*, *T. coincyi*, *T. elodes* and other species of the genus, we found no significant sequence variability (data not shown). Since plastidial markers failed to provide any evolutionary insights, with the results of our molecular phylogeny, chromosome counting and genome size analyses, we consider it more appropriate to support the nomenclatural combinations proposed by Vargas and Luceño (Sanchez-Villegas et al. 2022). They suggested combinations based on a few but solid distinctive morphological traits (see before in this paper), proposing a separation of *T. coincyi* and *T. elodes* at the rank of subspecies. Here, we propose the recognition of *T. balbisaniana* (DC.) Holub subsp. *balbisaniana* as

the nominal subspecies comprising all the populations ranging on the Maritime Alps and of the following subspecies which can accommodate the two Iberian taxa: *Tephroseris balbisiana* (DC.) Holub subsp. *coincy* (Rouy) P. Vargas and Luceño, and *Tephroseris balbisiana* (DC.) Holub subsp. *elodes* (Boiss. ex DC.) P. Vargas and Luceño.

Reevaluation of the status of the taxa and implementation of appropriate conservation policies are required. From a biodiversity conservation perspective, the current geographic isolation of the Iberian lineages, lasting since LGM, is particularly noteworthy in light of the potential adaptive or extinction rates facing future climate changes.

Supplementary Information The online version contains supplementary material available at <https://doi.org/10.1007/s00035-023-00300-w>.

Acknowledgements We thank Lenka Martonfiová for chromosome counting. As well, we are in debt with Jesus del Río and José Algarra for field works on *T. elodes*. Seeds of *T. coincy* were provided by Banco de Germoplasma Vegetal-Universidad Politécnica de Madrid “César Gómez Campo” (ESP003), Accession number: BGV-UPM 7610. We thank Izai Kikuchi for the English review of the manuscript. The authors acknowledge the support of NBFC to University of Torino (DBIOS), funded by the Italian Ministry of University and Research, PNRR, Missione 4 Componente 2, “Dalla ricerca all’impresa”, Investimento 1.4, Project CN00000033.

Funding Open access funding provided by Università degli Studi di Torino within the CRUI-CARE Agreement.

Data availability The sequences are publicly available on NCBI. Coordinates used in species distribution models are not published due to the rarity of the plants studied, but can be requested to the authors.

Declarations

Conflict of interest The authors declare that they have no known competing financial interests or personal relationships that could have appeared to influence the work reported in this paper.

Open Access This article is licensed under a Creative Commons Attribution 4.0 International License, which permits use, sharing, adaptation, distribution and reproduction in any medium or format, as long as you give appropriate credit to the original author(s) and the source, provide a link to the Creative Commons licence, and indicate if changes were made. The images or other third party material in this article are included in the article’s Creative Commons licence, unless indicated otherwise in a credit line to the material. If material is not included in the article’s Creative Commons licence and your intended use is not permitted by statutory regulation or exceeds the permitted use, you will need to obtain permission directly from the copyright holder. To view a copy of this licence, visit <http://creativecommons.org/licenses/by/4.0/>.

References

- Adamo M, Mammola S, Noble V, Mucciarelli M (2020) Integrating multiple lines of evidence to explore intraspecific variability in a rare endemic alpine plant and implications for its conservation. *Plants* 9:1160
- Aedo C (2019) *Tephroseris* (Rchb.) Rchb. *Flora Iber XVI (III) Compos (partim)* 1498–1503
- Alarcón M, Vargas P, Sáez L, Molero J, Aldasoro JJ (2012) Genetic diversity of mountain plants: two migration episodes of Mediterranean *Erodium* (Geraniaceae). *Mol Phylogenet Evol* 63:866–876
- Allouche O, Tsoar A, Kadmon R (2006) Assessing the accuracy of species distribution models: prevalence, kappa and the true skill statistic (TSS). *J Appl Ecol* 43:1223–1232
- Altınordu F, Martin E, Hamzaoglu E, Çetin Ö (2014) New chromosome counts, karyotype analyses and asymmetry indices in some taxa of genus *Senecio* L. and related genera *Tephroseris* (Rchb.) Rchb. and *Turanecio* Hamzaoglu belong to tribe Senecioneae (Asteraceae) from Turkey. *Plant Syst Evol* 300:2205–2216
- Araujo MB, Pearson RG, Thuiller W, Erhard M (2005) Validation of species–climate impact models under climate change. *Glob Change Biol* 11:1504–1513
- Baldwin BG, Markos S (1998) Phylogenetic utility of the external transcribed spacer (ETS) of 18S–26S rDNA: congruence of ETS and ITS trees of *Calycadenia* (Compositae). *Mol Phylogenet Evol* 10:449–463
- Bartolucci F, Peruzzi L, Galasso G et al (2018) An updated checklist of the vascular flora native to Italy. *Plant Biosyst* 152:179–303
- Birks HH (2008) The late-quaternary history of arctic and alpine plants. *Plant Ecol Divers* 1:135–146
- Blanca G, Cueto M (1992) In *Numeros cromosomáticos de plantas occidentales*. *Ann Jard Bot Madrid* 50:83
- Bobo-Pinilla J, Salmerón-Sánchez E, Mendoza-Fernández AJ et al (2022) Conservation and phylogeography of plants: from the Mediterranean to the rest of the world. *Diversity* 14:78
- Bonafede F, Vigonelli M, Alessandrini A (2013) *Tephroseris balbisiana* (DC.) Holub. In: *Actaplantarum Notes I*. ArabAFenice, 82
- Bono G (1967) Nota sui raggruppamenti a “*Senecio balbisianus*” DC e “*Peucedanum ostruthium*” Koch. del versante italiano del Massiccio cristallino dell’Argentera. *Nuovo Giorn Bot Ital NS* 101:409
- Boucher FC, Thuiller W, Roquet C et al (2012) Reconstructing the origins of high-alpine niches and cushion life form in the genus *Androsace* s.l. (Primulaceae). *Evol Int J Org Evol* 66:1255–1268
- Bouckaert R, Vaughan TG, Barido-Sottani J et al (2019) BEAST 2.5: an advanced software platform for Bayesian evolutionary analysis. *PLOS Comput Biol* 15:e1006650. <https://doi.org/10.1371/journal.pcbi.1006650>
- Braunisch V, Coppes J, Arlettaz R et al (2013) Selecting from correlated climate variables: a major source of uncertainty for predicting species distributions under climate change. *Ecography (cop)* 36:971–983. <https://doi.org/10.1111/j.1600-0587.2013.00138.x>
- Brun P, Thuiller W, Chauvier Y, Pellissier L, Wüest RO, Wang Z, Zimmermann NE (2020) Model complexity affects species distribution projections under climate change. *J Biogeogr* 47:130–142
- Cañadas EM, Fenu G, Peñas J et al (2014) Hotspots within hotspots: endemic plant richness, environmental drivers, and implications for conservation. *Biol Conserv* 170:282–291. <https://doi.org/10.1016/j.biocon.2013.12.007>
- Chater AO, Walters SM (1976) *Senecio* L. *Flora Eur* 4:191–205
- Christie C, Caetano S, Aeschmann D, Kropf M, Diadema K, Naciri Y (2014) The intraspecific genetic variability of siliceous and calcareous *Gentiana* species is shaped by contrasting demographic and re-colonization processes. *Mol Phylogenet Evol* 70:323–336
- Cornuet J-M, Santos F, Beaumont MA et al (2008) Inferring population history with DIYABC: a user-friendly approach to approximate Bayesian computation. *Bioinformatics* 24:2713–2719
- Cornuet J-M, Ravigné V, Estoup A (2010) Inference on population history and model checking using DNA sequence and microsatellite data with the software DIYABC (v1. 0). *BMC Bioinf* 11:1–11
- Cornuet J-M, Pudlo P, Veyssier J et al (2014) DIYABC v2.0: a software to make approximate Bayesian computation inferences about

- population history using single nucleotide polymorphism, DNA sequence and microsatellite data. *Bioinformatics* 30:1187–1189
- Cufodontis G (1933) Kritische Revision von *Senecio* sect. *Tephroseris* Beih Reper Spec Nov Regni Veg 70:
- Darriba D, Taboada GL, Doallo R, Posada D (2012) JModelTest 2: more models, new heuristics and parallel computing. *Nat Methods* 9:772
- Diadema K, Bretagnolle F, Affre L, Yuan YM, Médail F (2005) Geographic structure of molecular variation of *Gentiana ligustica* (Gentianaceae) in the Maritime and Ligurian regional hotspot, inferred from ITS sequences. *Taxon* 54:887–894
- Dixon CJ, Schönswetter P, Vargas P, Ertl S, Schneeweiss GM (2009) Bayesian hypothesis testing supports long-distance Pleistocene migrations in a European high mountain plant (*Androsace vitaliana*, Primulaceae). *Mol Phylogenet Evol* 53:580–591
- Doležel J, Greilhuber J, Suda J (2007) Estimation of nuclear DNA content in plants using flow cytometry. *Nat Protoc* 2:2233–2244
- Edgar RC (2004) MUSCLE: multiple sequence alignment with high accuracy and high throughput. *Nucleic Acids Res* 32(5):1792–1797. <https://doi.org/10.1093/nar/gkh340>
- Ehlers J, Ehlers J, Gibbard PL, Hughes PD (2011) Quaternary glaciations—extent and chronology: a closer look. Elsevier
- Fagundes NJR, Ray N, Beaumont M et al (2007) Statistical evaluation of alternative models of human evolution. *Proc Natl Acad Sci* 104:17614–17619
- Fick SE, Hijmans RJ (2017) WorldClim 2: new 1-km spatial resolution climate surfaces for global land areas. *Int J Climatol* 37:4302–4315. <https://doi.org/10.1002/joc.5086>
- García-Ruiz JM, Valero-Garcés BL, Martí-Bono C, González-Sampériz P (2003) Asynchronicity of maximum glacier advances in the central Spanish Pyrenees. *J Q Sci* 18:61–72
- Gent PR, Danabasoglu G (2011) Response to increasing Southern Hemisphere winds in CCSM4. *J Clim* 24:4992–4998
- Givnish TJ (2010) Ecology of plant speciation. *Taxon* 59:1326–1366
- Goczał J, Oleksa A, Rossa R et al (2020) Climatic oscillations in Quaternary have shaped the co-evolutionary patterns between the Norway spruce and its host-associated herbivore. *Sci Rep* 10:1–14
- Gouy M, Guindon S, Gascuel O (2010) SeaView version 4: a multiplatform graphical user interface for sequence alignment and phylogenetic tree building. *Mol Biol Evol* 27:221–224
- Greiner R, Vogt R, Oberprieler C (2012) Phylogenetic studies in the polyploid complex of the genus *Leucanthemum* Mill (Compositae, Anthemideae) based on cpDNA sequence variation. *Plant Syst Evol* 298:1407–1414
- Guerrina M, Theodoridis S, Minuto L et al (2022) First evidence of post-glacial contraction of Alpine endemics: Insights from *Berardia subacaulis* in the European Alps. *J Biogeogr* 49:79–93
- Guisan A, Thuiller W, Zimmermann NE (2017) Habitat suitability and distribution models: with applications in R. Cambridge University Press
- Gutiérrez Carretero L, Fuentes Carretero J, Cueto Romero M, et al (2019) Top ten de las plantas más amenazadas de Andalucía Oriental: taxones endémicos y no endémicos. *Acta Bot Malacitana* 44:5–33. <https://doi.org/10.24310/abm.v44i0.5636>
- Hanley JA, McNeil BJ (1982) The meaning and use of the area under a receiver operating characteristic (ROC) curve. *Radiology* 143:29–36
- Harrison S, Noss R (2017) Endemism hotspots are linked to stable climatic refugia. *Ann Bot* 119:207–214
- Huelsenbeck JP, Ronquist F (2001) MrBayes: Bayesian inference of phylogenetic trees. *Bioinformatics* 17:754–755
- Jayasena AS, Fisher MF, Panero JL et al (2017) Stepwise evolution of a buried inhibitor peptide over 45 My. *Mol Biol Evol* 34:1505–1516. <https://doi.org/10.1093/molbev/msx104>
- Jukes TH, Cantor CR et al (1969) Evolution of protein molecules. *Mamm Protein Metab* 3:21–132
- Kadereit JW, Laux P, Dillenberger MS (2021) A conspectus of *Tephroseris* (Asteraceae: Senecioneae) in Europe outside Russia and notes on the decline of the genus. *Willdenowia* 51:271–317
- Kadereit JW (2023) Adaptive evolutionary divergence of populations persisting in warming cold-stage refugia: candidate examples from the periphery of the European Alps. *Alp Bot* 133:1–10. <https://doi.org/10.1007/s00035-022-00291-0>
- Kochjarová J (2005) *Scilla bifolia* group in the Western Carpathians and adjacent part of the Pannonian lowland: annotated chromosome counts. *Preslia* 77:317–326
- Kumar S, Stecher G, Suleski M, Hedges SB (2017) TimeTree: a resource for timelines, timetrees, and divergence times. *Mol Biol Evol* 34:1812–1819
- Liu Y, Yang QE (2011) Cytology and its systematic implications in *Sinosenecio* (Senecioneae-Asteraceae) and two closely related genera. *Plant Syst Evol* 291:7–24
- Loidi J, Campos JA, Herrera M, Biurrun I, García-Mijangos I, García-Baquero G (2015) Eco-geographical factors affecting richness and phylogenetic diversity patterns of high-mountain flora in the Iberian Peninsula. *Alp Bot* 125:137–146
- Markos S, Baldwin BG (2001) Higher-level relationships and major lineages of *Lessingia* (Compositae, Astereae) based on nuclear rDNA internal and external transcribed spacer (ITS and ETS) sequences. *Syst Bot* 26:168–183
- Martín-Bravo S, Valcárcel V, Vargas P, Luceño M (2010) Geographical speciation related to Pleistocene range shifts in the western Mediterranean mountains (*Reseda* sect. *Glaucoreseda*, *Resedaceae*). *Taxon* 59:466–482
- Martínez-García F (2008) Catálogos de amenaza vs catálogos de protección. El ejemplo de *Senecio coincyi*. *Conserv Veg* 12:18
- Martínez-García F, Guerrero-García S, Pérez-García F (2012) Evaluation of reproductive success and conservation strategies for *Senecio coincyi* (Asteraceae), a narrow and threatened species. *Aust J Bot* 60:517–525
- Médail F, Baumel A (2018) Using phylogeography to define conservation priorities: the case of narrow endemic plants in the Mediterranean Basin hotspot. *Biol Conserv* 224:258–266
- Médail F, Diadema K (2009) Glacial refugia influence plant diversity patterns in the Mediterranean Basin. *J Biogeogr* 36:1333–1345. <https://doi.org/10.1111/j.1365-2699.2008.02051.x>
- Médail F, Quezel P (1997) Hot-spots analysis for conservation of plant biodiversity in the Mediterranean Basin. *Ann Missouri Bot Gard* 84:112. <https://doi.org/10.2307/2399957>
- Medail F, Quezel P (1999) Biodiversity hotspots in the Mediterranean Basin: setting global conservation priorities. *Conserv Biol* 13:1510–1513
- Molero J, Marfil JM (2017) Betic and Southwest Andalusia. The Vegetation of the Iberian Peninsula. Springer, New York, pp 143–247
- Molina-Venegas R, Aparicio A, Lavergne S, Arroyo J (2017) Climatic and topographical correlates of plant palaeo- and neoendemism in a Mediterranean biodiversity hotspot. *Ann Bot* 119:229–238
- Murín A (1960) Substitution of cellophane for glass covers to facilitate preparation of permanent squashes and smears. *Stain Technol* 35:351–353
- Nieto Feliner G, Cellinese N, Crowl AA, Frajman B (2023) Editorial: understanding plant diversity and evolution in the Mediterranean Basin. *Front Plant Sci* 14:1152340
- Noble V, Diadema K (2011) La flore des Alpes-Maritimes et de la Principauté de Monaco. Naturalia Publications, Turriers
- Nordenstam B (2007) Senecioneae. In: Kadereit JW, Jeffrey C (eds) The families and genera of vascular plants, flowering plants. Eudicots. Asterales, vol 8. Springer, Berlin, pp 208–241

- Nordenstam B, Pelser PB (2011) Notes on the generic limits of *Sinosenecio* and *Tephrosieris* (Compositae-Senecioneae)
- Olšavská K, Šingliarová B, Kochjarova J et al (2015) Exploring patterns of variation within the central-European *Tephrosieris longifolia* agg.: karyological and morphological study. *Preslia* 87:163–194
- Otto-Bliesner BL, Joussaume S, Braconnot P, et al (2009) Modeling and data syntheses of past climates: paleoclimate modeling inter-comparison Project Phase II Workshop; Estes Park, Colorado, 15--19 Sept= 2008
- Owens HL, Campbell LP, Dornak LL et al (2013) Constraints on interpretation of ecological niche models by limited environmental ranges on calibration areas. *Ecol Modell* 263:10–18
- Padilla-García N, Machon N, Segarra-Moragues JG, Martínez-Ortega MM (2021) Surviving in southern refugia: the case of *Veronica aragonensis*, a rare endemic from the Iberian Peninsula. *Alp Bot* 131:161–175
- Parisod C (2022) Plant speciation in the face of recurrent climate changes in the Alps. *Alp Bot* 132:21–28
- Pellissier L, Bräthen KA, Vittoz P et al (2013) Thermal niches are more conserved at cold than warm limits in arctic-alpine plant species. *Glob Ecol Biogeogr* 22:933–941
- Pelser PB, Nordenstam B, Kadereit JW, Watson LE (2007) An ITS phylogeny of tribe Senecioneae (Asteraceae) and a new delimitation of *Senecio* L. *Taxon* 56:1077–1104
- Pelser PB, Kennedy AH, Tepe EJ, et al (2010) Patterns and causes of incongruence between plastid and nuclear Senecioneae (Asteraceae) phylogenies. *Am J Botany* 97:856–873. <https://doi.org/10.3732/ajb.0900287>
- Peñas J, Cañadas E, Del Rio J (2019) Fitogeografía de Sierra Nevada e implicaciones para la conservación. *Biol la Conserv plantas en Sierra Nevada Principios y retos para su Preserv*. Universidad de Granada, Granada, pp 81–116
- Peredo EL, Revilla MÁ, Jiménez-Alfaro B et al (2009) Historical biogeography of a disjunctly distributed, Spanish alpine plant, *Senecio boissieri* (Asteraceae). *Taxon* 58:883–892
- Pignatti S, Guarino R, La Rosa M (2017) *Flora d'Italia*, 2nd edn. Edagricole Calderini, Bologna
- Rouy MG (1890) Diagnoses de plantes nouvelles pour la flore européenne. *Bull La Société Bot Fr* 37:162–168
- Ren C, Hong Y, Wang L, Yang Q-E (2017) Generic recircumscription of *Parasenecio* (Asteraceae: Senecioneae) based on nuclear ribosomal and plastid DNA sequences, with descriptions of two new genera. *Bot J Linn Soc* 184:418–443. <https://doi.org/10.1093/botlinnean/box034>
- Sánchez-Villegas RS, de la Peña BQ, Villegas MS et al (2022) Novedades corológicas y nomenclaturales para la flora vascular de la Sierra de Gredos (Sistema Central), III. *Flora Montiberica* 82:24–30
- Sandel B, Arge L, Dalsgaard B et al (2011) The influence of late quaternary climate-change velocity on species endemism. *Science* (80-) 334:660–664
- Schmitt T, Muster C, Schönswetter P (2010) Are disjunct alpine and arctic-alpine animal and plant species in the western Palearctic really “relics of a cold past”? Relict species: phylogeography and conservation biology. Springer, Berlin Heidelberg, pp 239–252
- Schönswetter P, Suda J, Popp M et al (2007) Circumpolar phylogeography of *Juncus biglumis* (Juncaceae) inferred from AFLP fingerprints, cpDNA sequences, nuclear DNA content and chromosome numbers. *Mol Phylogenet Evol* 42:92–103
- Skokanová K, Šingliarová B, Kochjarová J, Paule J (2019) Nuclear ITS and AFLPs provide surprising implications for the taxonomy of *Tephrosieris longifolia* agg. and the endemic status of *T. longifolia* subsp. *moravica*. *Plant Syst Evol* 305:865–884
- Stamatakis A (2014) RAxML version 8: a tool for phylogenetic analysis and post-analysis of large phylogenies. *Bioinformatics* 30:1312–1313. <https://doi.org/10.1093/bioinformatics/btu033>
- StatSoft Incorporated (2013) *Electronic Statistics Textbook*. StatSoft, Tulsa. <http://www.statsoft.com/textbook>
- Stucky BJ (2012) SeqTrace: a graphical tool for rapidly processing DNA sequencing chromatograms. *J Biomol Tech JBT* 23:90
- Taberlet P, Fumagalli L, Wust-Saucy A-G, Cosson J-F (1998) Comparative phylogeography and postglacial colonization routes in Europe. *Mol Ecol* 7:453–464
- Talavera G, Castresana J (2007) Improvement of phylogenies after removing divergent and ambiguously aligned blocks from protein sequence alignments. *Syst Biol* 56:564–577
- Thompson JD (1999) Population differentiation in Mediterranean plants: insights into colonization history and the evolution and conservation of endemic species. *Heredity* (edinb) 82:229–236. <https://doi.org/10.1038/sj.hdy.6885040>
- Thuiller W, Georges D, Gueguen M, et al (2021) biomod2: ensemble platform for species distribution modeling
- Tutin TG, Heywood VH, Burges NA et al (1980) *Flora Europaea*. Cambridge University Press, Cambridge
- Vargas P (2003) Molecular evidence for multiple diversification patterns of alpine plants in Mediterranean Europe. *Taxon* 52:463–476
- Wang L-Y, Pelser PB, Nordenstam B et al (2009) Strong incongruence between the ITS phylogeny and generic delimitation in the nemosenecio-sinosenecio-tephrosieris assemblage (Asteraceae: Senecioneae). *Bot Stud* 50:435–442
- Wasof S, Lenoir J, Aarrestad PA et al (2015) Disjunct populations European vascular plant species keep the same climatic niches. *Glob Ecol Biogeogr* 24:1401–1412
- Watanabe S, Hajima T, Sudo K et al (2011) MIROC-ESM 2010: model description and basic results of CMIP5-20c3m experiments. *Geosci Model Dev* 4:845–872
- White TJ, Bruns T, Lee S et al (1990) Amplification and direct sequencing of fungal ribosomal RNA genes for phylogenetics. *PCR Protoc Guid Methods Appl* 18:315–322
- Xu T, Shi Z, An Z (2018) Responses of ENSO and NAO to the external radiative forcing during the last millennium: results from CCSM4 and MPI-ESM-P simulations. *Quat Int* 487:99–111
- Zizka A, Carvalho FA, Calvente A et al (2020) No one-size-fits-all solution to clean GBIF. *PeerJ* 8:e9916
- Zuur AF, Ieno EN (2016) A protocol for conducting and presenting results of regression-type analyses. *Methods Ecol Evol* 7:636–645

Publisher's Note Springer Nature remains neutral with regard to jurisdictional claims in published maps and institutional affiliations.